The Astrophysical Journal, 690:1303–1312, 2009 January 10 doi:10.1088/0004-637X/690/2/1303


# THE EXCEPTIONALLY LUMINOUS TYPE II-LINEAR SUPERNOVA 2008es

A. A. Miller, R. Chornock, D. A. Perley, M. Ganeshalingam, W. Li, N. R. Butler[1], J. S. Bloom[2], N. Smith, M. Modjaz, D. Poznanski, A. V. Filippenko, C. V. Griffith, J. H. Shiode, and J. M. Silverman
Department of Astronomy, University of California, Berkeley, CA 94720-3411, USA; amiller@astro.berkeley.edu
*Received 2008 August 18; accepted 2008 September 3; published 2008 December 12*

## ABSTRACT

We report on our early photometric and spectroscopic observations of the extremely luminous Type II supernova (SN) 2008es. SN 2008es, with an observed peak optical magnitude of $m_V = 17.8$ and at a redshift $z = 0.213$, has a peak absolute magnitude of $M_V = -22.3$, making it the second most luminous SN ever observed. The photometric evolution of SN 2008es exhibits a fast decline rate ($\sim 0.042$ mag d$^{-1}$), similar to the extremely luminous Type II-Linear (II-L) SN 2005ap. We show that SN 2008es spectroscopically resembles the luminous Type II-L SN 1979C. Although the spectra of SN 2008es lack the narrow and intermediate-width line emission typically associated with the interaction of an SN with the circumstellar medium of its progenitor star, we argue that the extreme luminosity of SN 2008es is powered via strong interaction with a dense, optically thick circumstellar medium. The integrated bolometric luminosity of SN 2008es yields a total radiated energy at ultraviolet and optical wavelengths of $\gtrsim 10^{51}$ erg. Finally, we examine the apparently anomalous rate at which the Texas Supernova Search has discovered rare kinds of SNe, including the five most luminous SNe observed to date, and find that their results are consistent with those of other modern SN searches.

*Key words:* supernovae: general – supernovae: individual (SN 2008es)

*Online-only material:* color figures

## 1. INTRODUCTION

Wide-field synoptic optical imaging surveys are continuing to probe the parameter space of time-variable phenomena with increasing depth and temporal coverage (e.g., Becker et al. 2004; Morales-Rueda et al. 2006; Bramich et al. 2008), unveiling a variety of transients ranging from the common (Rau et al. 2008) to the unexplained (e.g., Barbary et al. 2008). Untargeted ("blind") synoptic wide-field imaging surveys, such as the Texas Supernova Search (TSS; Quimby 2006) conducted with the ROTSE-III 0.45 m telescope (Akerlof et al. 2003), have uncovered a large number of rare transients, including the four most luminous supernovae (SNe) observed to date: SN 2005ap (Quimby et al. 2007), SN 2008am (Yuan et al. 2008a), SN 2006gy (Ofek et al. 2007; Smith et al. 2007, 2008b), and SN 2006tf (Smith et al. 2008a). Observations of these very luminous events are starting to allow the detailed physical study of the extrema in core-collapse SNe. They appear to be powered in part by their interaction with a highly dense circumstellar medium (CSM; see Smith et al. 2008a, and references therein), though other possibilities have been advanced. Clearly, the discovery of more such events would allow an exploration of the variety of the phenomenology as related to the diversity of progenitors and CSM.

Recently, the TSS discovered yet another luminous transient on 2008 April 26.23 (UT dates are used throughout this paper), which they suggested was a variable active galactic nucleus at a redshift $z = 1.02$ (Yuan et al. 2008b). Gezari & Halpern (2008) then hypothesized that the transient was a flare from the tidal disruption of a star by a supermassive black hole. Miller et al. (2008) first identified SN 2008es as potentially an extremely luminous Type II SN (see also Gezari et al. 2008a), and we later definitively confirmed this with further spectroscopic observations (Chornock et al. 2008a); the event was assigned the name SN 2008es by the IAU (Chornock et al. 2008b). It is located at $\alpha = 11^{\rm h}56^{\rm m}49\overset{\rm s}{.}06$, $\delta = +54^\circ27'24\overset{''}{.}77$ (J2000.0).

Here we present our analysis of SN 2008es, which is classified as a Type II-Linear (II-L) SN based on the observed linear (in mag) decline in the photometric light curve (Barbon et al. 1979; Doggett & Branch 1985). At $z = 0.213$, SN 2008es has a peak optical magnitude of $M_V = -22.3$; among SNe, this is second only to SN 2005ap. Aside from the extreme luminosity, SN 2008es is of great interest since detailed UV through IR observations provide a unique opportunity to study the mass-loss properties of an evolved post-main-sequence massive star via its interaction with the surrounding dense CSM. A similar analysis of SN 2008es has been presented by Gezari et al. (2008b).

The outline of this paper is as follows. We present our observations in Section 2, and the photometric and spectroscopic analyses of this and public (NASA) data in Sections 3 and 4, respectively. A discussion is given in Section 5, and our conclusions are summarized in Section 6. Throughout this paper we adopt a concordance cosmology of $H_0 = 70$ km s$^{-1}$ Mpc$^{-1}$, $\Omega_{\rm M} = 0.3$, and $\Omega_\Lambda = 0.7$.

## 2. OBSERVATIONS

Here we present our ground-based optical and near-IR (NIR) photometry and optical spectroscopy, along with space-based *Swift* UV, optical, and X-ray observations. NIR photometry of SN 2008es was obtained simultaneously in $J$, $H$, and $K_s$ with the Peters Automated Infrared Imaging Telescope (PAIRITEL; Bloom et al. 2006) beginning 2008 May 16. To improve the photometric signal-to-noise ratio (S/N), we stacked images over multiple nights. For the $K_s$ images the S/N of the SN remained low, despite the stacks made over multiple epochs, and therefore we do not include these data in our subsequent analysis. Aperture photometry, using a custom pipeline, was used to measure the $J$ and $H$ magnitudes of the isolated SN

[1] *Gamma-Ray Large Area Space Telescope* (*GLAST*) Fellow.
[2] Sloan Research Fellow.

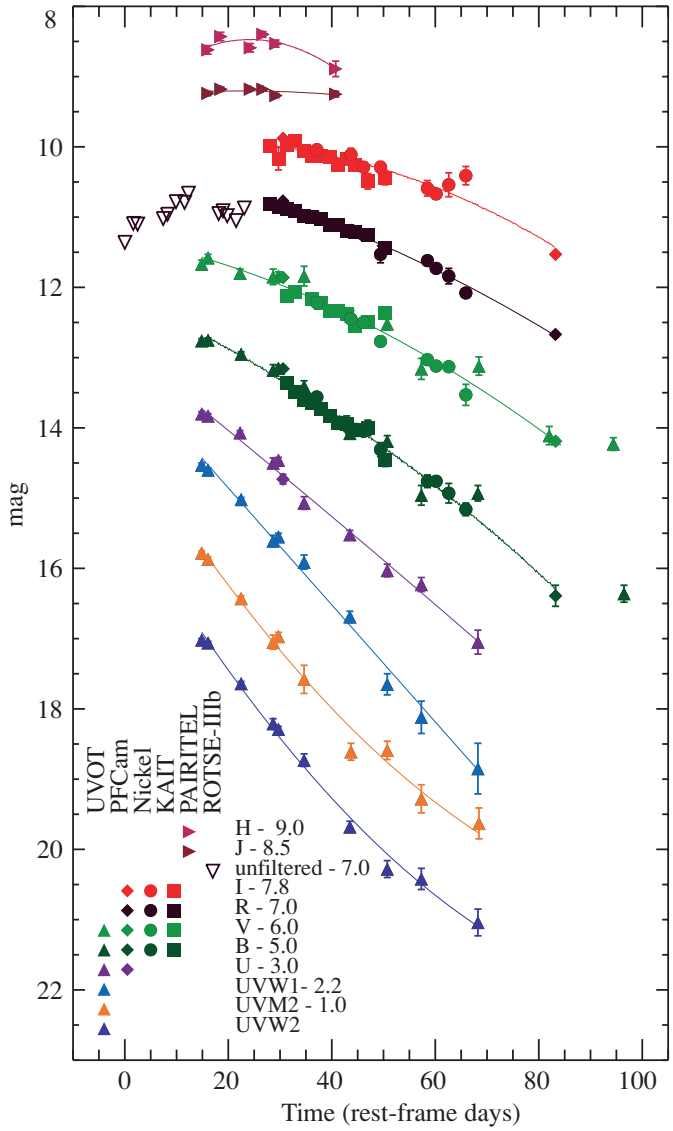


**Figure 1.** Observed UV-optical-NIR light curves of SN 2008es. The data have not been corrected for Galactic or host-galaxy extinction. We include ROTSE-IIIb unfiltered observations from the literature (open symbols; Gezari et al. 2008b), as well as our optical-NIR observations (filled symbols; KAIT, Nickel, PFCam, and PAIRITEL) and space-based UVOT observations from *Swift* (filled triangles). We adopt the discovery date of SN 2008es, 2008 April 26.23, as "day 0" for this SN. Low-order polynomial fits to each band have been overplotted to help guide the eye.

(A color version of this figure is available in the online journal.)

calibrated to the Two Micron All Sky Survey catalog (see Bloom et al. 2008). The resulting light curves are presented in Figure 1. The final PAIRITEL photometry is reported in Table 1.

Optical photometry of SN 2008es was obtained in *BVRI* with the Katzman Automatic Imaging Telescope (KAIT; Filippenko et al. 2001) and the 1 m Nickel telescope at Lick Observatory beginning 2008 May 30. Point-spread function (PSF)-fitting photometry was performed on the SN and several comparison stars using the IRAF/DAOPHOT package (Stetson 1987) and transformed into the Johnson–Cousins system. Calibrations for the field were obtained with the Nickel telescope on three photometric nights. The final photometry from KAIT and the Nickel telescope is given in Tables 2 and 3, respectively.

Additional optical photometry was obtained in *UBVRI* on 2008 June 2 and *BVRI* on 2008 August 5 with PFCam on the 3 m

**Table 1**
PAIRITEL Observations of SN 2008es

| $t_{mid}$[a] (days) | Obs. Window[b] (days) | Filter | Exp. Time (s) | Mag[c] |
|---|---|---|---|---|
| 4602.24 | 2.06 | *J* | 2895.91 | 17.74 ± 0.03 |
| 4605.28 | 6.09 | *J* | 3869.06 | 17.68 ± 0.03 |
| 4612.17 | 2.09 | *J* | 4606.78 | 17.68 ± 0.02 |
| 4615.15 | 6.08 | *J* | 6458.90 | 17.68 ± 0.02 |
| 4618.19 | 2.19 | *J* | 6129.29 | 17.77 ± 0.03 |
| 4632.17 | 6.04 | *J* | 4944.24 | 17.75 ± 0.04 |
| 4602.24 | 2.06 | *H* | 2880.22 | 17.62 ± 0.06 |
| 4605.27 | 6.09 | *H* | 3751.34 | 17.43 ± 0.06 |
| 4612.17 | 2.09 | *H* | 4598.93 | 17.59 ± 0.06 |
| 4615.15 | 6.08 | *H* | 6451.06 | 17.40 ± 0.04 |
| 4618.19 | 2.19 | *H* | 6074.35 | 17.53 ± 0.05 |
| 4632.17 | 6.04 | *H* | 4865.76 | 17.89 ± 0.11 |

**Notes.** PAIRITEL observations were stacked over multiple epochs to increase the S/N.
[a] Mid-point between the first and last exposures in a single stacked image, reported as JD−2,450,000.
[b] Time between the first and last exposures in a single stacked image.
[c] Observed value; not corrected for Galactic extinction.

Shane telescope at the Lick Observatory. The data were reduced using standard techniques and aperture photometry was used to extract the SN flux. *BVRI* calibrations were done using the same stars as those used for the Nickel and KAIT observations. Calibrations for the *U* band were not obtained with the Nickel telescope. Therefore, we convert the Sloan Digital Sky Survey (SDSS) colors of stars in the field to the *U* band with the color transformations of Jester et al. (2005), and use these stars for our *U*-band calibration. The final PFCam photometry is reported in Table 4.

The *Swift* satellite observed SN 2008es during 13 epochs between 2008 May 14 and August 21. We downloaded the Ultraviolet/Optical Telescope (UVOT; Roming et al. 2005) data from the *Swift* data archive and analyzed the Level 2 sky image data in *U*, *B*, and *V* according to the photometry calibration and recipe by Li et al. (2006). The *Swift* UV filters (*UVW*1, *UVM*1, and *UVW*2) were reduced following Poole et al. (2008). The final *Swift* UVOT photometry is reported in Table 5.

Simultaneous observations of SN 2008es occurred with the *Swift* X-ray Telescope (XRT; Burrows et al. 2005), for which we confirm a nondetection of X-ray emission (see also Gezari & Halpern 2008). To place a limit on the source flux we assume a power-law spectrum with a photon index $\Gamma = 2$, absorbed by elements associated with Galactic H I. We took an extraction region of radius 64 pixels (∼2.′5) and fit the PSF model around the centroid of the optical emission. We obtain a $3\sigma$ limiting flux of $9 \times 10^{-15}$ erg cm$^{-2}$ s$^{-1}$ in the 0.3–10 keV band for a total exposure of 54.7 ks. This represents an upper limit to the X-ray luminosity of SN 2008es of $\sim 1.2 \times 10^{42}$ erg s$^{-1}$.

We obtained spectra of SN 2008es on 2008 May 16.3, 2008 May 29.3, and 2008 July 7.3 using the Kast spectrograph on the Lick 3 m telescope (Miller & Stone 1993). Additional spectra were obtained on 2008 June 7.4 and 2008 August 3.3 using the low-resolution imaging spectrometer on the Keck I 10 m telescope (Oke et al. 1995) and on 2008 June 21.2 and 2008 June 23.2 using the R. C. Spectrograph on the Kitt Peak 4 m telescope, following the approval of our request for Kitt Peak Director's Discretionary Time. The spectra were extracted and calibrated following standard procedures (e.g., Matheson et al. 2000). Clouds were present during several of the observations, making the absolute flux scales unreliable. The spectrograph

**Table 2**
KAIT Observations of SN 2008es

| $t_{obs}$[a] (days) | Filter | Exp. Time (s) | Mag[b] |
|---|---|---|---|
| 4620.72 | *B* | 360.00 | 18.36 ± 0.04 |
| 4622.73 | *B* | 360.00 | 18.49 ± 0.05 |
| 4624.72 | *B* | 360.00 | 18.60 ± 0.04 |
| 4626.72 | *B* | 360.00 | 18.64 ± 0.06 |
| 4628.72 | *B* | 360.00 | 18.73 ± 0.07 |
| 4630.72 | *B* | 360.00 | 18.83 ± 0.06 |
| 4632.74 | *B* | 360.00 | 18.93 ± 0.09 |
| 4634.77 | *B* | 360.00 | 18.94 ± 0.11 |
| 4636.73 | *B* | 360.00 | 19.03 ± 0.09 |
| 4639.70 | *B* | 360.00 | 19.00 ± 0.11 |
| 4643.74 | *B* | 360.00 | 19.46 ± 0.09 |
| 4620.72 | *V* | 300.00 | 18.12 ± 0.06 |
| 4622.73 | *V* | 300.00 | 18.07 ± 0.03 |
| 4626.72 | *V* | 300.00 | 18.17 ± 0.04 |
| 4628.72 | *V* | 300.00 | 18.22 ± 0.04 |
| 4630.72 | *V* | 300.00 | 18.33 ± 0.04 |
| 4632.74 | *V* | 300.00 | 18.33 ± 0.06 |
| 4634.77 | *V* | 300.00 | 18.38 ± 0.09 |
| 4636.73 | *V* | 300.00 | 18.55 ± 0.03 |
| 4639.70 | *V* | 300.00 | 18.50 ± 0.04 |
| 4643.74 | *V* | 300.00 | 18.37 ± 0.05 |
| 4616.74 | *R* | 300.00 | 17.81 ± 0.03 |
| 4618.76 | *R* | 300.00 | 17.85 ± 0.04 |
| 4620.72 | *R* | 300.00 | 17.88 ± 0.04 |
| 4622.73 | *R* | 300.00 | 17.91 ± 0.03 |
| 4624.72 | *R* | 300.00 | 17.99 ± 0.04 |
| 4626.72 | *R* | 300.00 | 18.00 ± 0.03 |
| 4628.72 | *R* | 300.00 | 18.03 ± 0.04 |
| 4630.72 | *R* | 300.00 | 18.11 ± 0.05 |
| 4632.74 | *R* | 300.00 | 18.11 ± 0.03 |
| 4634.77 | *R* | 300.00 | 18.20 ± 0.04 |
| 4636.73 | *R* | 300.00 | 18.21 ± 0.05 |
| 4639.70 | *R* | 300.00 | 18.26 ± 0.05 |
| 4643.74 | *R* | 300.00 | 18.44 ± 0.06 |
| 4616.74 | *I* | 300.00 | 17.74 ± 0.07 |
| 4618.76 | *I* | 300.00 | 17.92 ± 0.16 |
| 4620.72 | *I* | 300.00 | 17.72 ± 0.05 |
| 4622.73 | *I* | 300.00 | 17.67 ± 0.05 |
| 4624.72 | *I* | 300.00 | 17.81 ± 0.05 |
| 4626.72 | *I* | 300.00 | 17.88 ± 0.04 |
| 4628.72 | *I* | 300.00 | 17.88 ± 0.05 |
| 4630.72 | *I* | 300.00 | 17.90 ± 0.07 |
| 4632.74 | *I* | 300.00 | 18.01 ± 0.06 |
| 4634.77 | *I* | 300.00 | 17.93 ± 0.07 |
| 4636.73 | *I* | 300.00 | 18.01 ± 0.08 |
| 4639.70 | *I* | 300.00 | 18.24 ± 0.11 |
| 4643.74 | *I* | 300.00 | 18.20 ± 0.09 |

**Notes.**
[a] Exposure midpoint, reported as JD−2,450,000.
[b] Observed value; not corrected for Galactic extinction.

**Table 3**
Nickel Observations of SN 2008es

| $t_{obs}$[a] (days) | Filter | Exp. Time (s) | Mag[b] |
|---|---|---|---|
| 4627.75 | *B* | 360.00 | 18.56 ± 0.02 |
| 4635.75 | *B* | 360.00 | 19.04 ± 0.07 |
| 4638.71 | *B* | 360.00 | 19.05 ± 0.03 |
| 4642.67 | *B* | 360.00 | 19.31 ± 0.10 |
| 4653.67 | *B* | 360.00 | 19.76 ± 0.09 |
| 4655.71 | *B* | 360.00 | 19.76 ± 0.04 |
| 4658.67 | *B* | 360.00 | 19.93 ± 0.14 |
| 4662.67 | *B* | 360.00 | 20.16 ± 0.09 |
| 4627.75 | *V* | 300.00 | 18.22 ± 0.03 |
| 4635.75 | *V* | 300.00 | 18.45 ± 0.04 |
| 4638.71 | *V* | 300.00 | 18.50 ± 0.03 |
| 4642.67 | *V* | 300.00 | 18.77 ± 0.04 |
| 4653.67 | *V* | 300.00 | 19.03 ± 0.04 |
| 4655.71 | *V* | 300.00 | 19.12 ± 0.04 |
| 4658.67 | *V* | 300.00 | 19.13 ± 0.07 |
| 4662.67 | *V* | 300.00 | 19.53 ± 0.15 |
| 4627.75 | *R* | 300.00 | 18.01 ± 0.02 |
| 4635.75 | *R* | 300.00 | 18.19 ± 0.04 |
| 4638.71 | *R* | 300.00 | 18.25 ± 0.03 |
| 4642.67 | *R* | 300.00 | 18.53 ± 0.12 |
| 4653.67 | *R* | 300.00 | 18.62 ± 0.04 |
| 4655.71 | *R* | 300.00 | 18.73 ± 0.03 |
| 4658.67 | *R* | 300.00 | 18.84 ± 0.11 |
| 4662.67 | *R* | 300.00 | 19.08 ± 0.05 |
| 4627.75 | *I* | 300.00 | 17.79 ± 0.04 |
| 4635.75 | *I* | 300.00 | 17.86 ± 0.09 |
| 4638.71 | *I* | 300.00 | 18.04 ± 0.04 |
| 4642.67 | *I* | 300.00 | 18.04 ± 0.08 |
| 4653.67 | *I* | 300.00 | 18.34 ± 0.11 |
| 4655.71 | *I* | 300.00 | 18.42 ± 0.07 |
| 4658.67 | *I* | 300.00 | 18.29 ± 0.17 |
| 4662.67 | *I* | 300.00 | 18.16 ± 0.13 |

**Notes.**
[a] Exposure midpoint, reported as JD−2,450,000.
[b] Observed value; not corrected for Galactic extinction.

**Table 4**
PFCam Observations of SN 2008es

| $t_{obs}$[a] (days) | Filter | Exp. Time (s) | Mag[b] |
|---|---|---|---|
| 4619.81 | *U* | 1230.00 | 17.73 ± 0.07 |
| 4619.83 | *B* | 630.00 | 18.16 ± 0.01 |
| 4683.70 | *B* | 360.00 | 21.39 ± 0.15 |
| 4619.83 | *V* | 930.00 | 17.86 ± 0.01 |
| 4683.71 | *V* | 360.00 | 20.19 ± 0.05 |
| 4619.79 | *R* | 930.00 | 17.77 ± 0.01 |
| 4683.68 | *R* | 600.00 | 19.67 ± 0.04 |
| 4619.85 | *I* | 1230.00 | 17.63 ± 0.01 |
| 4683.70 | *I* | 360.00 | 19.28 ± 0.03 |

**Notes.**
[a] Exposure midpoint, reported as JD−2,450,000.
[b] Observed value; not corrected for Galactic extinction.

slit was placed at the parallactic angle, so the relative spectral shapes should be accurate (Filippenko 1982), with the exception of the Kitt Peak spectra, which have a small amount of second-order light contamination at wavelengths longward of ∼8000 Å. The full SN 2008es spectral sequence is plotted in Figure 2. The two Kitt Peak spectra show little evolution in the two days that separate them and have been combined to increase the S/N (day 33 in Figure 2). A log of our spectroscopic observations is presented in Table 6.

We searched our spectra for the possible presence of narrow lines and were unable to positively identify any in either emission or absorption. Therefore, without a detection of the host galaxy, we determine the redshift of SN 2008es directly from the SN spectrum. As the SN aged, broad P-Cygni spectral features appeared, including an emission feature near 7900 Å that we identify as H$\alpha$ near a redshift of 0.2. Other spectral features are consistent with a Type II SN at about that redshift.

To get a more accurate redshift, we identified two similar reference spectra of the Type II-L SNe 1979C and 1980K from

**Table 5**
UVOT Observations of SN 2008es

| $t_{obs}$[a] (days) | Filter | Exp. Time (s) | Mag[b] |
|---|---|---|---|
| 4600.75 | *UVW2* | 1585.70 | 17.02 ± 0.02 |
| 4602.25 | *UVW2* | 1802.20 | 17.06 ± 0.02 |
| 4610.00 | *UVW2* | 2119.30 | 17.64 ± 0.03 |
| 4617.50 | *UVW2* | 542.40 | 18.21 ± 0.07 |
| 4618.75 | *UVW2* | 1731.10 | 18.29 ± 0.04 |
| 4624.75 | *UVW2* | 487.70 | 18.73 ± 0.09 |
| 4635.50 | *UVW2* | 1664.50 | 19.68 ± 0.08 |
| 4644.25 | *UVW2* | 1593.40 | 20.28 ± 0.12 |
| 4652.25 | *UVW2* | 1317.80 | 20.42 ± 0.15 |
| 4665.50 | *UVW2* | 1765.70 | 21.04 ± 0.19 |
| 4600.75 | *UVM2* | 1043.20 | 16.78 ± 0.03 |
| 4602.25 | *UVM2* | 1148.40 | 16.87 ± 0.03 |
| 4610.00 | *UVM2* | 1523.60 | 17.43 ± 0.04 |
| 4617.50 | *UVM2* | 338.60 | 18.05 ± 0.10 |
| 4618.75 | *UVM2* | 1110.60 | 17.97 ± 0.06 |
| 4624.75 | *UVM2* | 150.30 | 18.58 ± 0.20 |
| 4635.75 | *UVM2* | 1149.50 | 19.61 ± 0.12 |
| 4644.25 | *UVM2* | 1081.80 | 19.59 ± 0.13 |
| 4652.25 | *UVM2* | 938.10 | 20.28 ± 0.20 |
| 4665.75 | *UVM2* | 1071.50 | 20.63 ± 0.22 |
| 4600.75 | *UVW1* | 792.40 | 16.78 ± 0.03 |
| 4602.25 | *UVW1* | 900.70 | 16.85 ± 0.03 |
| 4610.00 | *UVW1* | 1058.30 | 17.27 ± 0.03 |
| 4617.50 | *UVW1* | 270.70 | 17.86 ± 0.08 |
| 4618.75 | *UVW1* | 865.10 | 17.80 ± 0.05 |
| 4624.75 | *UVW1* | 243.70 | 18.16 ± 0.10 |
| 4635.50 | *UVW1* | 831.80 | 18.94 ± 0.08 |
| 4644.25 | *UVW1* | 796.10 | 19.90 ± 0.15 |
| 4652.25 | *UVW1* | 790.00 | 20.37 ± 0.23 |
| 4665.50 | *UVW1* | 1048.30 | 21.10 ± 0.36 |
| 4600.75 | *U* | 395.80 | 16.80 ± 0.03 |
| 4602.25 | *U* | 449.90 | 16.83 ± 0.03 |
| 4609.75 | *U* | 399.60 | 17.07 ± 0.03 |
| 4617.50 | *U* | 134.90 | 17.50 ± 0.07 |
| 4618.75 | *U* | 431.90 | 17.46 ± 0.04 |
| 4624.75 | *U* | 121.50 | 18.07 ± 0.09 |
| 4635.50 | *U* | 415.40 | 18.52 ± 0.06 |
| 4644.25 | *U* | 397.40 | 19.03 ± 0.09 |
| 4652.25 | *U* | 386.70 | 19.23 ± 0.10 |
| 4665.50 | *U* | 523.60 | 20.05 ± 0.17 |
| 4600.75 | *B* | 395.80 | 17.76 ± 0.03 |
| 4602.25 | *B* | 449.90 | 17.75 ± 0.03 |
| 4610.00 | *B* | 527.80 | 17.95 ± 0.03 |
| 4617.50 | *B* | 135.00 | 18.18 ± 0.08 |
| 4618.75 | *B* | 431.90 | 18.15 ± 0.04 |
| 4624.75 | *B* | 121.60 | 18.41 ± 0.08 |
| 4635.50 | *B* | 415.40 | 19.08 ± 0.06 |
| 4644.25 | *B* | 397.50 | 19.19 ± 0.08 |
| 4652.25 | *B* | 328.60 | 19.96 ± 0.14 |
| 4665.50 | *B* | 523.70 | 19.93 ± 0.11 |
| 4699.75 | *B* | 4150.20 | 21.36 ± 0.12 |
| 4600.75 | *V* | 395.70 | 17.67 ± 0.06 |
| 4602.25 | *V* | 449.90 | 17.58 ± 0.05 |
| 4609.75 | *V* | 399.50 | 17.80 ± 0.06 |
| 4617.50 | *V* | 134.90 | 17.85 ± 0.11 |
| 4618.75 | *V* | 432.00 | 17.84 ± 0.06 |
| 4624.75 | *V* | 81.00 | 17.84 ± 0.14 |
| 4635.75 | *V* | 415.40 | 18.41 ± 0.08 |
| 4644.25 | *V* | 397.60 | 18.52 ± 0.09 |
| 4652.25 | *V* | 328.50 | 19.16 ± 0.15 |
| 4665.75 | *V* | 398.90 | 19.12 ± 0.13 |
| 4682.25 | *V* | 1876.40 | 20.11 ± 0.13 |
| 4697.25 | *V* | 4316.10 | 20.23 ± 0.09 |

**Notes.**
[a] Exposure midpoint, reported as JD−2,450,000.
[b] Observed value; not corrected for Galactic extinction.

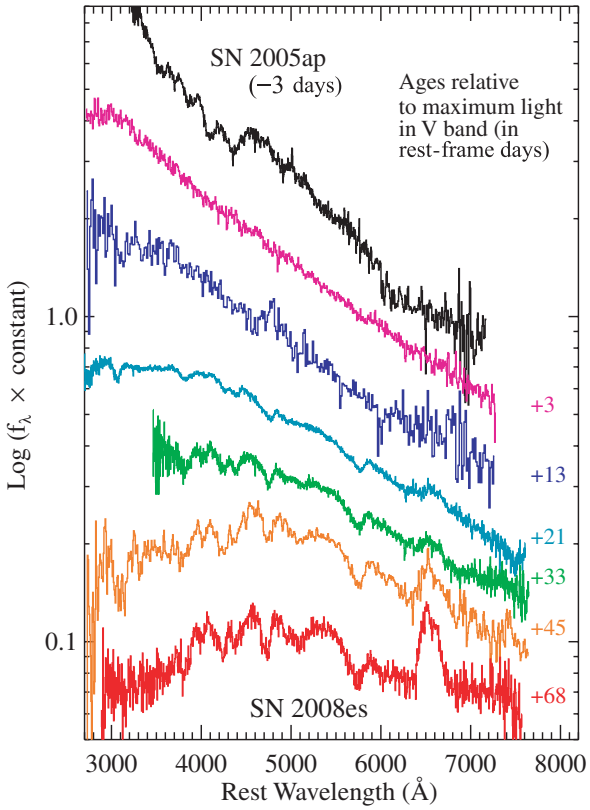


**Figure 2.** Spectral evolution of SN 2008es. Spectra of SN 2008es (in color) are labeled with their ages in the rest frame of the supernova ($z = 0.213$) relative to the observed *V*-band maximum on 2008 May 13.3. The spectra become progressively redder as the SN ages and broad P-Cygni spectral features become more prominent with time. By +68 days, a broad emission feature of H$\alpha$ is clearly present. The top spectrum (in black) is the earliest spectrum of SN 2005ap, the most luminous observed SN (Quimby et al. 2007).
(A color version of this figure is available in the online journal.)

**Table 6**
Log of Spectroscopic Observations

| Age[a] (days) | UT Date | Instrument[b] | Range (Å) | Exp. Time (s) | Seeing (″) | Air Mass | Photometric? (y/n) |
|---|---|---|---|---|---|---|---|
| 3 | 2008-05-16.345 | Kast | 3300–8830 | 1500 | 2.4 | 1.3 | y |
| 13 | 2008-05-29.253 | Kast | 3300–8820 | 1800 | 2.3 | 1.1 | n |
| 21 | 2008-06-07.399 | LRIS | 3200–9230 | 1200 | 1.6 | 2.0 | y |
| 33 | 2008-06-21.194 | RC | 4200–9280 | 1800 | 2.9 | 1.3 | y |
| 34 | 2008-06-23.189 | RC | 4200–9280 | 2400 | 1.8 | 1.3 | y |
| 45 | 2008-07-07.252 | Kast | 3300–9280 | 4200 | 2.5 | 1.6 | y |
| 68 | 2008-08-03.254 | LRIS | 3500–9190 | 877 | 0.9 | 2.0 | n |

**Notes.**
[a] Age in rest-frame days relative to the observed *V*-band maximum on 2008 May 13.3.
[b] Kast: Kast spectrograph on Lick 3 m telescope. LRIS: low resolution imaging spectrometer on Keck-I 10 m telescope. RC: R. C. Spectrograph on Kitt Peak 4 m telescope.

the literature (Branch et al. 1981; Uomoto & Kirshner 1986). These spectral comparisons are shown in the bottom panel of Figure 3. We used the SuperNova IDentification code of Blondin & Tonry (2007) to cross-correlate the day 68 spectrum of SN 2008es with the two reference spectra and derived a weighted-average $z = 0.213 \pm 0.006$, which we adopt throughout this paper. This redshift agrees with a fit to the broad H$\alpha$ emission line in the day 68 spectrum, which yields a flux centroid of $z = 0.210$. The SN 2008es redshift determined using this method is correlated with the expansion velocity, but we assume that the bias due to this effect is small given that all three SNe have H$\alpha$ emission lines of a similar width at late times.

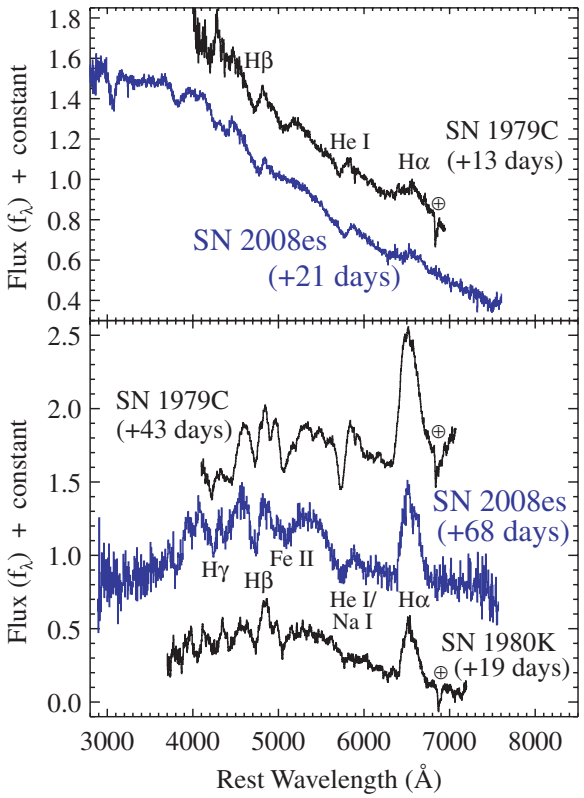


**Figure 3.** Spectral comparisons of SN 2008es to two SNe II-L. All spectra are labeled with their respective ages in rest-frame days relative to maximum light, and prominent spectral features are identified. The zero point of the flux scale is accurate for the SN 2008es spectra (in blue), while the comparison spectra (in black) are vertically offset. The top panel shows a comparison at an early epoch of SN 2008es with SN 1979C from 1979 April 28 (Branch et al. 1981). The bottom panel shows a comparison at a later epoch with SN 1979C from 1979 May 28 (Branch et al. 1981) and SN 1980K (spectra from 1980 November 15 and 17 combined; Uomoto & Kirshner 1986). Telluric absorption bands in the SNe 1979C and 1980K spectra are marked with a ⊕ symbol.

(A color version of this figure is available in the online journal.)

## 3. PHOTOMETRIC RESULTS

Our data set provides excellent broadband coverage of SN 2008es from the UV to the NIR, which allows us to model changes in the spectral energy distribution (SED). In order to sample each photometric band onto a single set of common epochs, we fit low-order polynomials to each light curve, which we then interpolate onto a common grid. NIR observations were only included on or around epochs where we detected the SN.

We create an SED at each of the common epochs and fit a single-component blackbody (BB) to the data following the procedure described by Modjaz et al. (2008). Prior to the SED/BB fits, we add a systematic term to the uncertainty in the photometric measurement in each band. This term is added in quadrature to the statistical uncertainty, and for the NIR (*JH*) is equal to 2%, in the optical (*BVRI*) we adopt 3%, while for *U* band we adopt 10%, and the adopted UV (*UVW*1, *UVM*2, *UVW*2) systematic uncertainty is 20%. Across all epochs of the BB fits the total $\chi^2$ per degree of freedom is 45.6/65, which suggests that our systematic terms may be slightly overestimated. We assume no host-galaxy extinction (for further details see Section 5), and correct our measurements for the modest amount of Galactic reddening $E(B-V) = 0.011$ mag (Schlegel et al. 1998). From the SED/BB fits we derive the temperature, radius, and luminosity of the SN as a function of time, as shown in Figure 4. The temperature and luminosity decrease while the radius increases with time, as expected for an expanding and cooling SN photosphere.

In order to determine the time of *V*-band maximum light, which at the redshift of this SN roughly corresponds to rest-frame *B*, we convert the early time *g*, *r*, and *i*′ photometry taken with the Palomar 1.5 m telescope from Gezari et al. (2008b) to *VRI* using the color equations from Jester et al. (2005). Following a quadratic fit to these data, we find that the observed *V*-band maximum occurred on ∼2008 May 13, ∼15 rest-frame days after discovery. The observed peak is $V = 17.8$ mag, which corresponds to $M_V = -22.3$ mag, with a scatter about our fit of 0.04 mag.

In Figure 5, we show two representative fits to the SED of SN 2008es at 26.6 and 65.4 rest-frame days after discovery. In all epochs we observe excess emission relative to a single BB in the bluest of the *Swift* filters, *UVW*2, while starting around 55 rest-frame days after discovery, there is excess emission in both *UVW*2 and *UVM*2. This excess was also observed in the Type II-Plateau (II-P) SN 2006bp, where it was attributed to complex line blanketing by Fe-peak elements (Immler et al. 2007). The blue excess is readily identified in the UV color curves (e.g., *UVW*2–*UVW*1) of SN 2008es, which evolve toward the red until ∼50 rest-frame days after discovery, at which point the *UVW*2–*UVW*1 and *UVM*2–*UVW*1 colors become progressively more and more blue. These points were excluded from our SED/BB fits. To confirm that we were not underestimating the bolometric luminosity of the SN, we directly integrated the flux in the SED using the same method as Modjaz et al. (2008). We show the results of this direct integration in the lower panel of Figure 4, and in all cases we find that the BB model and the direct integration method agree to within $\lesssim 20\%$.

The observed linear decline in the light curve of SN 2008es leads us to classify it as a Type II-L SN. We measure a bolometric photometric decay rate of 0.042 mag day$^{-1}$, which is slightly faster than the *V*-band (roughly rest-frame *B*) rate of 0.036 mag day$^{-1}$. This rate is also slightly slower than the rest-frame *B*-band decay of both SN 1979C (0.046 mag day$^{-1}$; Panagia et al. 1980) and SN 1980K (0.055 mag day$^{-1}$; Barbon et al. 1982). Furthermore, integrating the bolometric light curve from 15 to 83 rest-frame days after discovery yields a total radiated energy of $\sim 9 \times 10^{50}$ erg, comparable to the canonical $10^{51}$ erg deposited into the kinetic energy of a SN. If we assume the same bolometric correction factor to the observed *V*-band light curve both pre- and post-maximum, and if we include the early data from Gezari et al. (2008b), we find that the total radiated energy of SN 2008es over the first 83 days after discovery is $\sim 1.1 \times 10^{51}$ erg.

The three *Swift* UVOT observations taken more than 80 days after the discovery of SN 2008es show tentative evidence for a significant reduction in the SN photometric decline rate (see Figure 1). We note, however, that the late-time UVOT measurements have significant errors, and these observations may be consistent with the early trend seen in the light curve. Gezari et al. (2008b) suggested that these observations were evidence that the SN luminosity made a transition to being powered by radioactive heating from $^{56}$Co. With only two observations of this decline, we caution against prematurely identifying the $^{56}$Co decay tail, and instead argue that the observations are inconclusive at this time. For instance, it would be possible to mimic the behavior of $^{56}$Co decay with a late-time light echo, or interaction with an extended CSM. We note that SN 2006gy also showed evidence for a "flattening" several months after

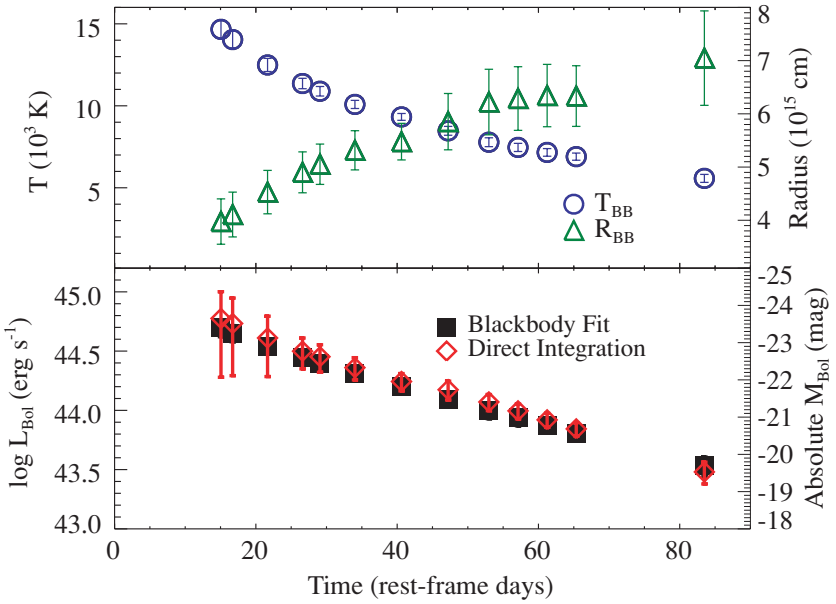


**Figure 4.** Photospheric and bolometric luminosity evolution of SN 2008es. Top: temperature evolution of SN 2008es based on BB fits (open circles) and inferred radius (open triangles). The error bars on the radius are likely to be slightly overestimated because the errors on the BB temperature and luminosity are correlated. Bottom: bolometric luminosity of SN 2008es derived via two independent methods, BB modeling (closed squares) and integration of the total UV+optical (+NIR where available) flux (open diamonds). The two methods agree to within $\lesssim 20\%$.

(A color version of this figure is available in the online journal.)

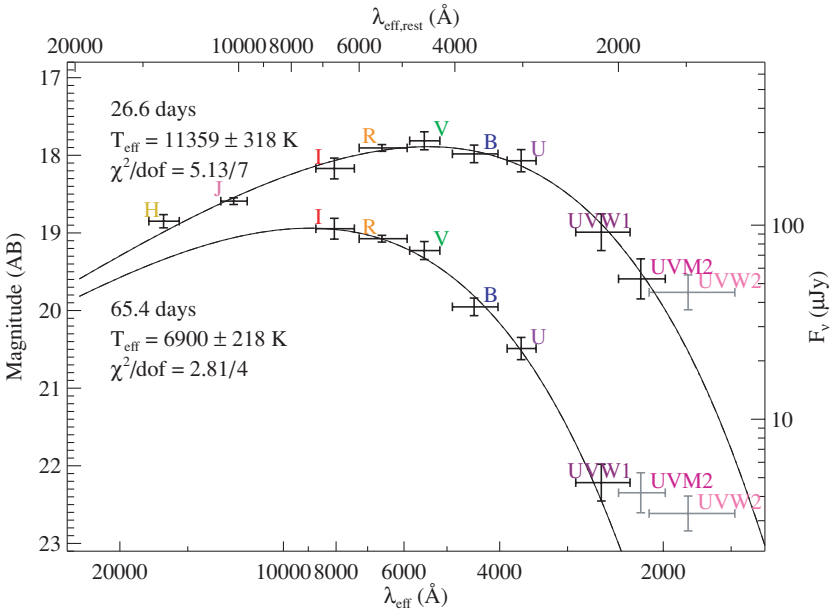


**Figure 5.** SEDs from SN 2008es corrected for Galactic extinction. We show two representative SEDs of SN 2008es at $\sim 27$ and $\sim 65$ rest-frame days after discovery. The SEDs are well fit by a single BB component. Note that relative to the model BB there is excess flux in the *UVW2* band in both epochs, while the *UVM2* band shows excess in the later epoch. All UV measurements that exhibit a clear excess relative to a BB are shown in gray and are excluded from the fits.

(A color version of this figure is available in the online journal.)

explosion (Smith et al. 2007), but further observations taken the following year indicated that this was not clearly the $^{56}$Co tail (Smith et al. 2008b). Our last optical spectrum (Figure 2) also shows no evidence that the ejecta were becoming optically thin on that date, as would be expected if SN 2008es were transitioning to the radioactive decay tail. Late-time photometry will be necessary to conclusively identify if and when the light curve of SN 2008es made a transition to being powered by $^{56}$Co decay, and thus allow a measurement of the amount of $^{56}$Ni synthesized in the explosion.

## 4. SPECTROSCOPY

The SN 2008es spectral sequence plotted in Figure 2 is labeled with ages (in the rest frame) relative to the observed *V*-band maximum in order to facilitate comparison with SNe 1979C and 1980K in Figure 3. Our first two spectra of SN 2008es (at +3 and +13 days relative to maximum light) show a smooth and featureless blue continuum with no identifiable spectral features. In particular, we do not detect an emission feature near 5650 Å (4660 Å in the rest frame) seen in earlier spectra of

SN 2008es taken between 2008 May 1 and 2008 May 8 (Yuan et al. 2008b; Gezari et al. 2008b). Gezari et al. (2008b) attribute this feature solely to He II λ4686, but we note that transient emission features seen in the early spectra of some SNe IIn at similar wavelengths are due to a combination of He II λ4686 and the Wolf–Rayet C III/N III λ4640 blend (Niemela, Ruiz, & Phillips 1985; Leonard et al. 2000).

In addition, the spectrum of the extremely luminous SN 2005ap from −3 days is shown at the top of Figure 2. The SN 2005ap spectrum is also very blue, but has additional spectral features that are not seen in our SN 2008es spectrum from a similar epoch. Quimby et al. (2007) identified the strongest spectral feature in SN 2005ap, the "W"-shaped feature near 4200 Å, as being due to a blend of C III, N III, and O III with an expansion velocity of about 20,000 km $s^{-1}$.

Our next spectrum, at +21 days is noticeably redder and is the first to show strong spectral features. Both SN 1979C at a similar epoch and SN 2008es show a blue continuum with weak, low-contrast lines of H and He I lines present mostly in absorption (Figure 3). However, Hα is present only in emission and is weak in SN 2008es. The Hα line in SN 2008es has a full width at half-maximum (FWHM) intensity of 10,000 km $s^{-1}$ and an equivalent width of only 22 Å (both of these values have large uncertainties due to difficulties in defining the continuum for a line with such a low amplitude). One difference between the two objects is the lower apparent velocities in SN 2008es. The Hβ and He I λ5876 lines of SN 1979C have absorption minima at velocities of 9700 and 8900 km $s^{-1}$, respectively. In SN 2008es, these values are 6000 and 5700 km $s^{-1}$, respectively, although we caution that the exact values are correlated with the assumed value for the redshift.

Over the next two months, the spectra of SN 2008es plotted in Figure 2 became redder, reflecting the cooling photospheric temperature evolution discussed above. In addition, the spectral features first seen in the day +21 spectrum gradually became more prominent. The SN features are still muted in amplitude relative to those expected in a normal Type II SN. This may be an example of the "top-lighting" effect described by Branch et al. (2000), where continuum emission from interaction with CSM illuminates the SN ejecta from above and results in a rescaling of the amplitudes of spectral features.

By the time of our day +68 spectrum, the P-Cygni spectral features due to H Balmer lines, Na I, and Fe II become more prominent and the overall appearance starts resembling that of normal SNe II. The Hα profile lacks an absorption component, which may be common to SNe II-L and not SNe II-P (e.g., Schlegel 1996; Filippenko 1997). The broad Hα emission extends (at zero intensity) from −9000 to 9000 km $s^{-1}$, with an FWHM of 9500 km $s^{-1}$. This velocity width is intermediate between that of the SNe 1979C and 1980K spectra (FWHM ≈ 10,600 and ≈ 8200 km $s^{-1}$, respectively).

Unlike in most core-collapse SNe, the velocity of the minimum of the Hβ line *increased* over time, from 6000 km $s^{-1}$ at day 21 to 8700 km $s^{-1}$ at day 68, as shown in the bottom panel of Figure 6. The exact values of the velocity depend directly on the assumed redshift, but the *trend* is independent of those uncertainties. Unfortunately, the other absorption lines are mostly blended (except for Hα, which does not show an absorption component), so we cannot isolate the velocity trend in other spectral features without spectral modeling. The top panel of Figure 6 shows the evolution of the He I λ5876/Na I λ5892 blend. At early times He I dominates the blend, and as the ejecta cool at later epochs Na I should dominate, resulting in an

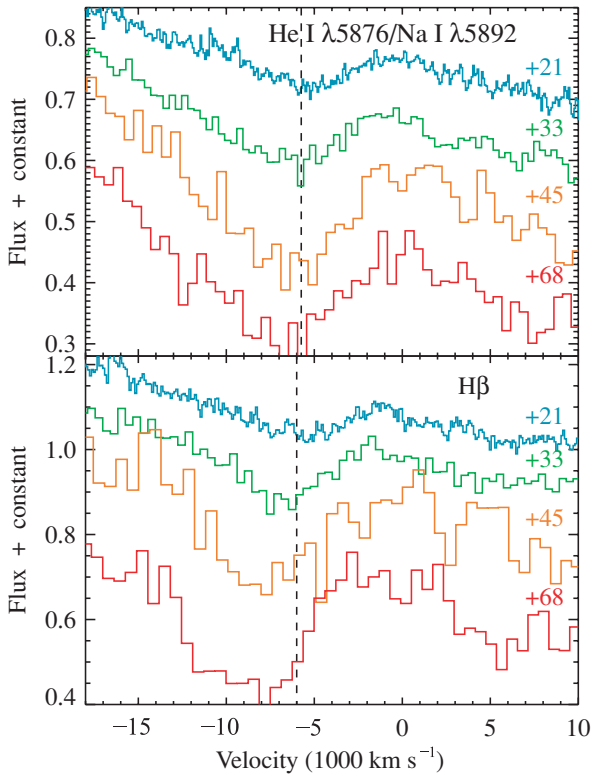


**Figure 6.** Velocity evolution of absorption minima. The spectra are labeled with dates after maximum light in the same manner as in Figure 2. In the bottom panel, the apparent blueshift of the Hβ absorption minimum increases over time. A vertical dashed line at −6000 km $s^{-1}$ marks the velocity of the absorption minimum on day 21 to guide the eye. In the top panel, the evolution of the He I λ5876/Na I λ5892 blend is plotted, with λ5876 used as the zero point of the velocity scale. The vertical dashed line at −5700 km $s^{-1}$ marks the absorption minimum on day 21 to guide the eye.

(A color version of this figure is available in the online journal.)

∼800 km $s^{-1}$ redward shift of the rest wavelength. After taking into account that redward shift, the top panel of Figure 6 also shows some weak evidence for a blueward shift of the absorption minimum to ∼8000 km $s^{-1}$.

The only SN known to us to show increasing absorption velocities over time is the peculiar SN Ib 2005bf. The trend of increasing absorption velocities was only visible in the three He I lines, but not in other lines such as Ca II H&K (Modjaz 2007). Tominaga et al. (2005) explained the effect as being due to progressive outward excitation of He I by radioactive $^{56}$Ni in the interior as the ejecta expanded and the density decreased, an effect that seems to be of little relevance to SN 2008es. A more likely possibility is that blending with some unidentified line is shifting the velocity of the apparent absorption minimum. At late times Hβ dominates its region of the spectrum, but at early times He II λ4686 could possibly be contributing emission to the blue wing of the Hβ absorption profile. Another scenario is that some unusual, but as yet unidentified, radiative transfer effect is affecting the wavelength of the apparent absorption minimum in SN 2008es. For example, if the optical depth in an optically thick line increases sufficiently rapidly with time (e.g., as the ejecta cool and recombine), then the apparent absorption minimum could move blueward (Jeffery & Branch 1990). None of these suggestions explain why such an effect would be present only in SN 2008es and not in normal SNe.

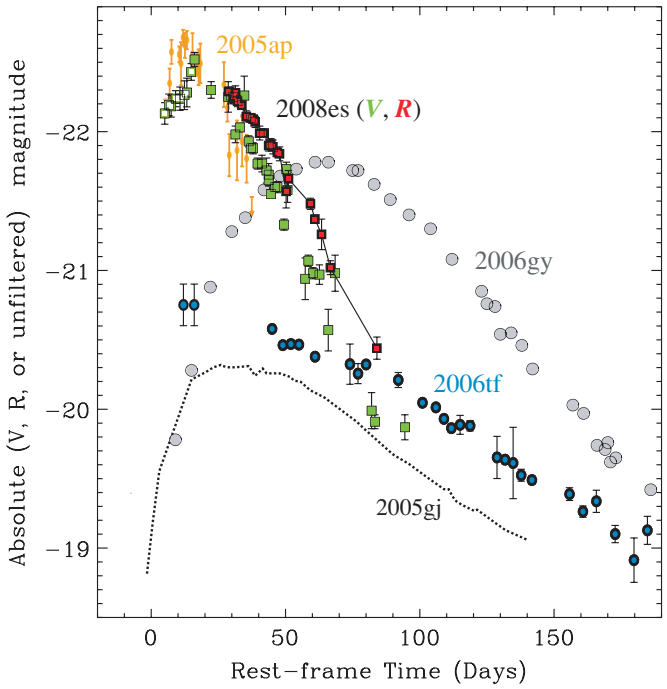


**Figure 7.** Rest-frame brightness evolution of five of the most luminous known SNe. For SN 2008es we derive the absolute magnitude using UVOT and the KAIT/Nickel *V*-band magnitudes (filled green squares) and the KAIT/Nickel *R*-band magnitudes (red squares), assuming that the discovery date is day 0. Early *g*-band photometry from Gezari et al. (2008b), converted to *V*-band using the color equations of Jester et al. (2005), is also shown (open green squares). The light curve for SN 2005ap (orange) is derived from unfiltered photometry in Quimby et al. (2007), and SN 2006gy (gray circles) is also unfiltered from Smith et al. (2007). *R*-band photometry of SN 2006tf (blue circles) is from Smith et al. (2008a), and $r/r'$ photometry of SN 2005gj (dotted line) is from Prieto et al. (2007). The light curve for SN 2006tf is shifted by +16 days from that in Smith et al. (2008a); since the explosion date is not known, we chose to align its time of peak luminosity with those of SNe 2005ap and 2008es.

(A color version of this figure is available in the online journal.)

## 5. DISCUSSION

### 5.1. The Physical Nature of SN 2008es

The photometric evolution of SN 2008es (see Figure 7) is much faster than that of other very luminous SNe such as SNe 2006gy (Smith et al. 2007; Ofek et al. 2007), 2006tf (Smith et al. 2008a), and 2005gj (Prieto et al. 2007), and its spectrum also betrays no evidence for the strong CSM interaction seen in these other SNe IIn, in the form of narrow lines from the CSM or intermediate-width H$\alpha$ from the post-shock shell. Indeed, considering both its photometric and spectroscopic evolution, we suggest that SN 2008es is most like the overluminous SN 2005ap (Quimby et al. 2007) and thereby most closely resembles a Type II-L that is 4–5 mag more luminous than typical SNe II-L (Richardson et al. 2002).

To power the tremendous luminosity of SN 2008es with radioactive decay would require an initial $^{56}$Ni mass of $\sim 10\,M_{\odot}$ (see e.g., Smith et al. 2007). This $^{56}$Ni mass would very likely need to be generated in a pair-instability explosion (Barkat et al. 1967; Bond et al. 1984), but this $^{56}$Ni mass seems problematic given that it would be larger than the modest envelope mass indicated by the relatively fast rise and decay time (see below). In addition, the photometric decline of 0.042 mag day$^{-1}$ is faster than that of $^{56}$Co, 0.0098 mag day$^{-1}$, making it unlikely that radioactive heating is the dominant source of the energy.

Despite the lack of a Type IIn spectrum, the most likely interpretation seems to be that the high luminosity of SN 2008es is the result of converting shock energy into visual light. This can be accomplished, in principle, if the shock kinetic energy is thermalized throughout a massive envelope, like a normal SN II-P or II-L, but with a much larger initial radius of (2–3) $\times 10^{15}$ cm (based on the peak luminosity and the evolution in Figure 4). Were the initial radius much smaller than this it would prove difficult to convert $\sim 10^{51}$ erg of kinetic energy to $\sim 10^{51}$ erg of radiation because there would be significant adiabatic losses. The apparent temperature evolution from $\sim$15,000 to 6000 K over a time period of $\sim$66 days (Figure 4), reminiscent of other normal SNe II, suggests that the recombination photosphere is receding through a cooling envelope in SN 2008es. In this scenario, the usual narrow/intermediate-width H$\alpha$ emission that is taken as a signpost of CSM interaction might be avoided if the CSM shell is initially very opaque, and if the shock encounters no further CSM at larger radii (see Smith et al. 2008a).

Since the required initial radius exceeds that of the largest known red supergiants (see Smith et al. 2001) by a factor of 20–30, it requires the envelope to be an unbound, opaque CSM shell ejected prior to the SN explosion instead of a traditional bound stellar envelope. Similar models were suggested for SN 2005ap (Quimby et al. 2007), SN 2006gy (Smith & McCray 2007), and SN 2006tf (Smith et al. 2008a), implying CSM envelope masses of 0.6, $\sim$10, and 18 $M_{\odot}$, respectively. The corresponding CSM mass for SN 2008es would be roughly $\sim 5\,M_{\odot}$ in this scenario, because its evolution and expansion speeds are slower than those of SN 2005ap. This CSM mass of $\sim 5\,M_{\odot}$ allows the observed H$\alpha$ Doppler velocities to remain faster than in SNe 2006gy and 2006tf, where the heavy CSM shells decelerated the shocks to only 4000 and 2000 km s$^{-1}$, respectively (Smith et al. 2007; Smith et al. 2008a). The smaller CSM mass for SN 2008es relative to SNe 2006gy and 2006tf would also explain the comparatively short rise and decay observed for SN 2008es, as the light diffusion time for this SN is much shorter than in SNe 2006gy and 2006tf (Smith & McCray 2007). The putative envelope ejection preceding SN 2008es must have occurred 10–100 yr prior to the explosion (for an unknown progenitor wind speed of $v_{\rm CSM} = 10$–100 km s$^{-1}$), indicating a progenitor mass-loss rate of order 0.05–0.5 $M_{\odot}$ yr$^{-1}$. This is much larger than any steady stellar wind (see Smith et al. 2007, and references therein), providing another case of impulsive mass ejection in the decades immediately preceding some SNe.

An alternative analysis of SN 2008es, submitted for publication shortly after this paper was made available electronically, also suggests that the extreme luminosity is powered via interaction with CSM (Gezari et al. 2008b). However, the initial version of Gezari et al. (2008b) argues against an unbound CSM shell ejected prior to the SN explosion, and instead argues that the CSM is created by a dense progenitor wind.

### 5.2. The Host of SN 2008es

Currently there is no conclusive detection of the host galaxy of SN 2008es, so its metallicity and corresponding implications for the pre-SN evolution are not known. From SDSS DR6 images (Adelman-McCarthy et al. 2008), we derive a 3$\sigma$ upper limit of $m_{r'} > 22.7$ mag at the SN position, which translates to roughly $M_V > -17.4$ mag at the SN redshift (neglecting any *K* corrections). Thus, the putative host galaxy is significantly less luminous than an $L_*$ galaxy and could be comparable

to or fainter than the Small Magellanic Cloud (with $M_V = -16.9$ mag).[3]

Without a definitive detection of the host galaxy we assume that there is no host extinction. This assumption is further supported by both the low luminosity of the host galaxy and our BB fits (see Section 3) that show excellent agreement with our UV measurements, where the effects of host extinction would be especially prominent. In analogy with the underluminous hosts of SNe 2006tf (Smith et al. 2008a) and 2005ap (Quimby et al. 2007), deep imaging after the SN has faded may uncover the host galaxy nearly coincident with the SN position, which would allow further constraints to be placed on extinction in the host. These three extreme SNe and their underluminous hosts may be hinting that very luminous SNe II preferentially occur in low-luminosity host galaxies.

### 5.3. Rates of Extremely Luminous SN 2008es-like Events

Over the past three years the TSS has successfully found tens of SNe with a surprising rate of unusual objects. The list of such SNe includes SN 2005ap, SN 2006gy, SN 2006tf, SN 2008am, and now SN 2008es. However, this apparent high anomaly rate is probably the result of combining a huge survey volume with an intrinsically rare class of objects. Following Quimby (2008), we compare the volume probed by the TSS for SNe Ia, and bright core-collapse SNe. The highest redshift of the ∼30 SNe Ia found by the TSS is $z \approx 0.1$, while SN 2005ap was found at $z \approx 0.3$. The comoving volume scanned by the TSS is therefore ∼23 times bigger for SN 2008es-like objects than for SNe Ia. Of the five bright objects found by the TSS, only two, SN 2005ap and SN 2008es, can be considered together as a class. Thus, the comparative rate is about $30/2 \times 23 \approx 350$ times smaller.

The KAIT SN search (Filippenko et al. 2001) has discovered about 400 SNe Ia in the past 10 years in targeted nearby galaxies, hence the expected number of SN 2008es-like objects is of order 1. This is consistent with the nondetection of any such SN.

Using the light curve of SN 2008es and the accumulated observations of about 10,000 spiral galaxies in the KAIT sample which were observed regularly during the past 10 years, we find an upper limit on the rate (per unit *K*-band luminosity) of such SNe to be about 1/160 times the local SN II rate (J. Leaman et al. 2009, in preparation). Furthermore, we note that if SN 2008es-like events preferentially occur in small, low-metallicity galaxies (see Section 5.2), the KAIT sample, which targets large, nearby galaxies, would be biased against the discovery of such an SN. While there are several SN search surveys with larger search volumes than the TSS, such as the SDSS-II Supernova Survey (Sako et al. 2008), the full details of these surveys (cadence, total survey volume, candidate SN color cuts, etc.) are not available at this time, and therefore we cannot directly compare them to the TSS. We conclude that the number of luminous Type II-L SNe, as discovered by the TSS, does not appear to be the result of a statistical fluke, and predict many such detections with future wide-field synoptic surveys.

## 6. CONCLUSIONS

We have reported on our early observations of SN 2008es, which at a peak optical magnitude of $M_V = -22.3$ is the second most luminous SN ever observed. We argue that the extreme luminosity of this SN was likely powered via strong interaction with a dense CSM, and that the steep decline in the light curve, 0.042 mag day$^{-1}$, indicates that the radioactive decay of $^{56}$Co is likely not the dominant source of energy for this SN. Integration of the bolometric light curve of SN 2008es yields a total radiated energy output of $\gtrsim 10^{51}$ erg. The optical spectra of SN 2008es resemble those of the luminous SN 1979C, but with an unexplained increase in the velocity of the H$\beta$ absorption minimum over time.

We also examined the rate of discovery of extremely luminous SNe by the Texas Supernova Search and find that their discovery of the five most luminous observed SNe in the past four years is probably not a fluke; several more such detections are expected in the coming years.

Finally, what behavior can we expect from SN 2008es at late times, roughly 1 year or more after discovery? Regardless of whether the peak luminosity was powered by radioactive decay or optically thick CSM interaction (see Smith et al. 2008b), a SN can be powered by strong CSM interaction at late times if the progenitor had a sufficiently high mass-loss rate in the centuries before exploding. We have seen examples of both: SN 2006tf had strong H$\alpha$ emission indicative of ongoing CSM interaction at late times (Smith et al. 2008a), whereas SN 2006gy did not (Smith et al. 2008b). SN 1979C was less luminous at peak than those two SNe, but it has been studied for three decades because its late-time CSM interaction is powering ongoing emission in the radio, optical, and X-ray (Weiler et al. 1981; Fesen & Matonick 1993; Immler et al. 1998). With such an extraordinarily high peak luminosity, a late-time IR echo such as that seen in SN 2006gy (Smith et al. 2008b) is also likely if SN 2008es has dust waiting at a radius of ∼0.3 pc. Alternatively, if SN 2008es were powered in whole or in part by radioactivity, a large mass of $^{56}$Ni should be evident in the late-time decline rate.

We thank the anonymous referee for comments that helped improve this paper. We are grateful to B. Jannuzi for approving Kitt Peak DD observations, and to Diane Harmer and David L. Summers for carrying out the observations. We wish to thank Neil Gehrels for his approval of the ToO requests for *Swift* observations, the *Swift* observing team for carrying out the observations, and J. Halpern, S. Gezari, and D. Grupe for the initial requests for *Swift* observations. M. Malkan accommodated a small telescope time trade, while N. Joubert and B. Macomber assisted with some of the observations. P. Nugent kindly checked for prediscovery images of SN 2008es from DeepSky. A.A.M. is supported by a UC Berkeley Chancellor's Fellowship. M.M. is supported by a Miller Institute research fellowship. N.R.B. and D.A.P. are partially supported by US Department of Energy SciDAC grant DE-FC02-06ER41453. J.S.B.'s group is partially supported by NASA/*Swift* grant NNG05GF55G and a Hellman Faculty Award. A.V.F.'s group is supported by the National Science Foundation (NSF) grant AST-0607485 and the TABASGO Foundation. The Peters Automated Infrared Imaging Telescope is operated by the Smithsonian Astrophysical Observatory (SAO) and was made possible by a grant from the Harvard University Milton Fund, the camera loan from the University of Virginia, and the continued support of the SAO and UC Berkeley. The PAIRITEL project is partially supported by NASA/*Swift* Guest Investigator Grant NNG06GH50G. KAIT and its ongoing operation were made possible by donations from Sun Microsystems, Inc., the Hewlett-Packard Company, AutoScope Corporation, Lick

[3] A galaxy ∼ 9″ to the northeast of the SN position is unlikely to be the host itself even if found to be at a similar redshift as SN 2008es; this would require significant massive star formation at a projected physical distance of ∼ 31 kpc.

Observatory, the NSF, the University of California, the Sylvia & Jim Katzman Foundation, and the TABASGO Foundation. We acknowledge the use of public data from the *Swift* data archive. Some of the data presented herein were obtained at the W. M. Keck Observatory, which is operated as a scientific partnership among the California Institute of Technology, the University of California, and NASA; the Observatory was made possible by the generous financial support of the W. M. Keck Foundation. The authors wish to recognize and acknowledge the very significant cultural role and reverence that the summit of Mauna Kea has always had within the indigenous Hawaiian community; we are most fortunate to have the opportunity to conduct observations from this mountain. We are grateful for the assistance of the dedicated staff at the Lick and Keck Observatories as well as at KPNO, PAIRITEL, and *Swift*.

## REFERENCES

Adelman-McCarthy, J. K., et al. 2008, ApJS, 175, 297
Akerlof, C. W., et al. 2003, PASP, 115, 132
Barbary, K., et al. 2008, ApJ, accepted, arXiv:0809.1648
Barbon, R., Ciatti, F., & Rosino, L. 1979, A&A, 72, 287
Barbon, R., Ciatti, F., & Rosino, L. 1982, A&A, 116, 35
Barkat, Z., Rakavy, G., & Sack, N. 1967, Phys. Rev. Lett., 18, 379
Becker, A. C., et al. 2004, ApJ, 611, 418
Blondin, S., & Tonry, J. L. 2007, ApJ, 666, 1024
Bloom, J. S., Starr, D. L., Blake, C. H., Skrutskie, M. F., & Falco, E. E. 2006, in Astronomical Data Analysis Software and Systems XV, ed. C. Gabriel, et al. (San Francisco, CA: ASP), 751
Bloom, J. S., et al. 2008, ApJ, accepted, arXiv:0803.3215
Bond, J. R., Arnett, W. D., & Carr, B. J. 1984, ApJ, 280, 825
Bramich, D. M., et al. 2008, MNRAS, 386, 887
Branch, D., Falk, S. W., Uomoto, A. K., Wills, B. J., McCall, M. L., & Rybski, P. 1981, ApJ, 244, 780
Branch, D., Jeffery, D. J., Blaylock, M., & Hatano, K. 2000, PASP, 112, 217
Burrows, D. N., et al. 2005, Space Sci. Rev., 120, 165
Chornock, R., Miller, A. A., Bloom, J. S., & Perley, D. A. 2008a, The Astronomer's Telegram, 1644, 1
Chornock, R., et al. 2008b, Central Bureau Electronic Telegrams, 1462
Doggett, J. B., & Branch, D. 1985, AJ, 90, 2303
Fesen, R. A., & Matonick, D. M. 1993, ApJ, 407, 110
Filippenko, A. V. 1982, PASP, 94, 715
Filippenko, A. V. 1997, ARA&A, 35, 309
Filippenko, A. V., Li, W. D., Treffers, R. R., & Modjaz, M. 2001, in IAU Colloq. 183, Small Telescope Astronomy on Global Scales, ed. B. Paczynski, W.-P. Chen, & C. Lemme (San Francisco, CA: ASP), 121
Gezari, S., & Halpern, J. P. 2008, The Astronomer's Telegram, 1524, 1
Gezari, S., et al. 2008a, The Astronomer's Telegram, 1578, 1
Gezari, S., et al. 2008b, ApJ, accepted, arXiv:0808.2812
Immler, S., Pietsch, W., & Aschenbach, B. 1998, A&A, 331, 601
Immler, S., et al. 2007, ApJ, 664, 435
Jeffery, D. J., & Branch, D. 1990, in Jerusalem Winter School for Theoretical Physics: Supernovae, ed. J. C. Wheeler, T. Piran, & S. Weinberg (Singapore: World Scientific), 149
Jester, S., et al. 2005, AJ, 130, 873
Leonard, D. C., Filippenko, A. V., Barth, A. J., & Matheson, T. 2000, ApJ, 536, 239
Li, W., Jha, S., Filippenko, A. V., Bloom, J. S., Pooley, D., Foley, R. J., & Perley, D. A. 2006, PASP, 118, 37
Matheson, T., Filippenko, A. V., Ho, L. C., Barth, A. J., & Leonard, D. C. 2000, AJ, 120, 1499
Miller, J. S., & Stone, R. P. S. 1993, in Lick Observatory Technical Reports 66, (Santa Cruz, CA: Lick Obs.)
Miller, A. A., et al. 2008, The Astronomer's Telegram, 1576, 1
Modjaz, M. 2007, PhD thesis, Harvard Univ.
Modjaz, M., et al. 2008, ApJ, submitted, arXiv:0805.2201
Morales-Rueda, L., Groot, P. J., Augusteijn, T., Nelemans, G., Vreeswijk, P. M., & van den Besselaar, E. J. M. 2006, MNRAS, 371, 1681
Niemela, V. S., Ruiz, M. T., & Phillips, M. M. 1985, ApJ, 289, 52
Ofek, E. O., et al. 2007, ApJ, 659, L13
Oke, J. B., et al. 1995, PASP, 107, 375
Panagia, N., et al. 1980, MNRAS, 192, 861
Poole, T. S., et al. 2008, MNRAS, 383, 627
Prieto, J. L., et al. 2007, AJ, submitted, arXiv:0706.4088
Quimby, R. 2006, BAAS, 38, 1216
Quimby, R. M. , et al. 2008, in New Horizons in Astronomy: Frank N. Bash Symposium 2007, ed. A. Frebel (San Francisco, CA: ASP)
Quimby, R. M., Aldering, G., Wheeler, J. C., Höflich, P., Akerlof, C. W., & Rykoff, E. S. 2007, ApJ, 668, L99
Rau, A., Ofek, E. O., Kulkarni, S. R., Madore, B. F., Pevunova, O., & Ajello, M. 2008, ApJ, 682, 1205
Richardson, D., Branch, D., Casebeer, D., Millard, J., Thomas, R. C., & Baron, E. 2002, AJ, 123, 745
Roming, P. W. A., et al. 2005, Space Sci. Rev., 120, 95
Sako, M., et al. 2008, AJ, 135, 348
Schlegel, E. M. 1996, AJ, 111, 1660
Schlegel, D. J., Finkbeiner, D. P., & Davis, M. 1998, ApJ, 500, 525
Smith, N., Chornock, R., Li, W., Ganeshalingam, M., Silverman, J. M., Foley, R. J., Filippenko, A. V., & Barth, A. J. 2008a, ApJ, 686, 467
Smith, N., Humphreys, R. M., Davidson, K., Gehrz, R. D., Schuster, M. T., & Krautter, J. 2001, AJ, 121, 1111
Smith, N., & McCray, R. 2007, ApJ, 671, L17
Smith, N., et al. 2007, ApJ, 666, 1116
Smith, N., et al. 2008b, ApJ,, 686, 485
Stetson, P. B. 1987, PASP, 99, 191
Tominaga, N., et al. 2005, ApJ, 633, L97
Uomoto, A., & Kirshner, R. P. 1986, ApJ, 308, 685
Weiler, K. W., van der Hulst, J. M., Sramek, R. A., & Panagia, N. 1981, ApJ, 243, 151
Yuan, F., Quimby, R., McKay, T., Chamarro, D., Sisson, M. D., Akerlof, C., & Wheeler, J. C. 2008b, The Astronomer's Telegram, 1515, 1
Yuan, F., et al. 2008a, The Astronomer's Telegram, 1389, 1